UNIVERSITY OF CALIFORNIA, SAN DIEGO

Power Maximization in Wave-Energy Converters Using Sampled-Data Extremum Seeking

A Thesis submitted in partial satisfaction of the

requirements for the degree

Master of Science

in

Mechanical Engineering

by

Tianjia Chen

Committee in charge:

Professor Sonia Martinez, Chair
Professor Jorge Cortes
Professor Robert Bitmead

2013

The Thesis of Tianjia Chen is approved, and it is acceptable in quality and form for publication on microfilm and electronically:

Chair

University of California, San Diego

2013

TABLE OF CONTENTS

LIST OF FIGURES

LIST OF TABLES

ACKNOWLEDGEMENTS

First, I would like to thank my advisor, Professor Sonia Martinez, for her generous support and guidance throughout the years of my graduate study. It is one of my most precious experiences as well as a great honor to have the opportunity to work with her. Through this period, not only do I benefit from her rich knowledge, I am also inspired by her strong personalities. I can still remember the persistent guidance she gave, even during her pregnancy. Besides, the ways of creative and critical thinking I learnt from her will be a huge fortune in my future.

I must also acknowledge my co-worker, Mr. Hamed Foroush, for his help and collaboration, especially his guidance in paper writing. His warmth and patience impressed me a lot and I was really encouraged in some difficult time throughout the research.

Last but not least, I want to thank my mother, my father and my grandparents, for their great support and care, as well as tremendous understanding, during the years of my graduate study in the United States, distant with them.

Chapter 2, in full, has been submitted for publication of the material as it may appear in proceedings of the 2014 American Control Conference, Portland, OR, June 2014, Tianjia Chen, Hamed Foroush and Sonia Martinez. The thesis author was the primary investigator and author of this paper.

Chapter 3, in part, has been submitted for publication of the material as it may appear in proceedings of the 2014 American Control Conference, Portland, OR, June 2014, Tianjia Chen, Hamed Foroush and Sonia Martinez. The thesis author was the primary investigator and author of this paper.

Chapter 4, in part, has been submitted for publication of the material as it may appear in proceedings of the 2014 American Control Conference, Portland, OR, June 2014, Tianjia Chen, Hamed Foroush and Sonia Martinez. The thesis author was the primary investigator and author of this paper.

Chapter 5, in part, has been submitted for publication of the material as it

may appear in proceedings of the 2014 American Control Conference, Portland, OR, June 2014, Tianjia Chen, Hamed Foroush and Sonia Martinez. The thesis author was the primary investigator and author of this paper.

ABSTRACT OF THE THESIS

Power Maximization in Wave-Energy Converters
Using Sampled-Data Extremum Seeking

by

Tianjia Chen

Master of Science in Mechanical Engineering

University of California, San Diego, 2013

Professor Sonia Martinez, Chair

Ocean waves bear huge, largely untapped energy which has drawn people's attention in recent decades. With the technology of wave-energy converters(WECs), the extraction of wave energy involves the process of energy conversion, which relates to the concern of efficiency as well as the constraints it introduces. In this work, we consider the problem of power maximization in wave-energy converters modeled as point-absorbers.

We focus on the method of sampled-data extremum-seeking, where we

give assumptions based on which the semiglobal practical asymptotic stability of the interconnected system is characterized. It is worth noting that the novelty lies in our assumptions on the discrete-time class of systems and constrained control inputs.

Besides the exploration in the theoretical aspect, we also propose the Numerical Extremum-Seeking (NES) algorithm for the plant of WEC. We prove that it is capable of solving the power maximization problem while ensuring the stability of the system. The analysis of NES algorithm is based on the aforementioned theory along with a Poincaré map technique and a gradient-projection method. Finally, we show the functionality of the proposed algorithm in simulation results. In addition to the regular-wave condition, we present the simulation for a more practical scenario, i.e., the irregular-wave case.

Chapter 1

Introduction

1.1 Motivation

Ocean power is a largely untapped, clean energy resource. Compared to wind energy, the main advantage of wave energy is its high spatial density and temporal persistence, which can make it more reliable. Wave-energy extraction and converters have drawn a huge attention over the past decades [5, 6]. The extraction of wave energy involves a chain of energy conversion processes, each of which is characterized by its efficiency as well as the constraints it introduces. In particular, novel mechanisms, sensors, and control techniques are necessary in order to harness wave energy more effectively. Motivated by this problem, this thesis studies the application of a sampled-data extremum-seeking technique for point-absorber *Wave-Energy Converters* (WECs).

For WECs, energy conversion occurs more efficiently when the undamped natural frequency of the device is close to the dominant frequency of the incident wave [9], while the velocity of the point-absorber is in phase with the excitation force of the incoming wave. A first relevant control strategy is the so-called *reactive control*, which aims to tune the dynamic parameters of the converter using controlled actuation [10]. However, reactive control may result in a negative mechanical spring, which has some practical issues [6]. Alternatively, the *latching control* strategy [4], aims to latch and release the device intermittently to achieve the approximate optimal phase control—regardless of the higher natural frequency of the device than wave frequency. Latching control usually relies on relatively heavy computations, and requires the prediction of the incoming wave some time into the future [6]. *Extremum seeking* (ES) is an adaptive control strategy for tracking a time-varying extremum, i.e., maximum or minimum, of an unknown, or poorly known cost function [1]. Amongst various ES approaches, the method of using sinusoidal perturbation to probe the system has been studied in [1]. Recently, a perturbation-based, discrete-time ES approach has been proposed to deal with the optimization problem of wave energy absorption by point absorbers [7], however this scheme does not account for possible constraints in their inputs. Alternatively, sampled-data ES relies on the tools of nonlinear programming [15], where the extremum is being searched *numerically* [17]. The first uniform treatment of such sampled-data ES scheme is studied in [15], whilst a different approach from the perspective of interconnected systems is presented in [11]. Both works provide a set of sufficient conditions for the closed-loop stability of generic sampled-data ES schemes. While the results of [15] apply to a general sampled-data ES scheme, [11] characterizes stability employing Lyapunov arguments for interconnected systems. This relates more directly to the structural features of the subsystems involved, which allows the more explicit identification of how problem parameters affect their performance. More recently, there is research [8] on the unified frameworks for sampled-data ES control. Opposed to the Lyapunov-based stability analysis in [15] and [11], trajectory-based proof is provided in [8]to carry out the stability property.

In this thesis, we propose a sampled-data numerical ES (NES) algorithm to maximize the power output via tuning the control parameter of the WEC according to the measured outputs. The advantage of our approach is that it handles constrained control inputs, by incorporating a projection method into the numerical algorithm. We then analyze the performance of such method under the assumption of a regular wave regime. In our WEC application, we encounter a similar interconnected stability problem as in [11], however, this time, with respect to a limit cycle. Thus, we extend their results to discrete-time systems configuration where, in addition, the control input is constrained to be in a compact set. Based on the extended results, the stability property of the limit cycle is characterized regarding the interconnection of the WEC plant and the proposed algorithm through a Poincaré map technique. Simulation results are provided to demonstrate the practicality of our proposed approach under both regular and irregular waves.

1.2 Thesis Structure

The thesis is organized as follows. In Chapter 2, we introduce the model of WEC as a point-absorber and formulate the optimization problem that we have studied in this thesis. Then, in Chapter 3, we present briefly the theory on the stability of sampled-data ES, where the contents are kept at an abstract level to be served in upcoming parts. In Chapter 4, a sampled-data NES algorithm is proposed and the relevant stability property when interconnected with the WEC model is studied, comprehensively. The simulation results are given in Chapter 5, which is followed by the conclusions.

Chapter 2

Problem Formulation

2.1 Point-Absorber Model of the WEC

We model the Wave Energy Converter (WEC) as a point absorber in heave motion (one degree of freedom) with a Power Take-Off (PTO) mechanism, see Figure 2.1.

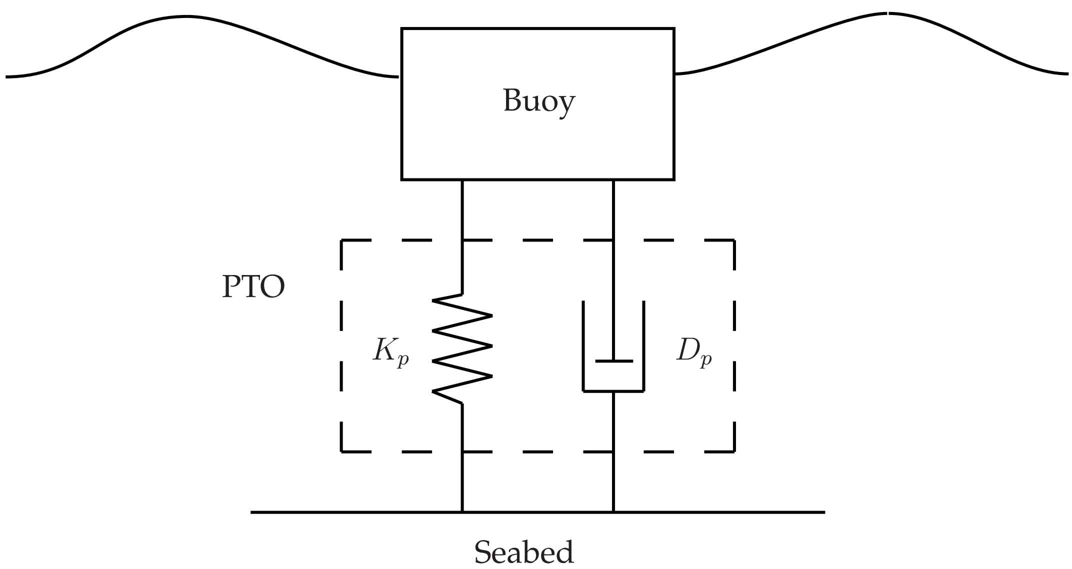

Figure 2.1: Schematic model of a heaving point absorber

Using q to denote the displacement of the buoy away from its equilibrium position and ω for the incoming wave frequency, the WEC dynamic model can be described by (refer to [14, 12, 6])

$$(M_s + M_a(\omega))\ddot{q} + D_h(\omega)\dot{q} + K_h q = f_e + f_p, \tag{2.1}$$

where M_s and $M_a(\omega)$ denote respectively the structural mass of the buoy and the added mass caused by the inertia of the water surrounding it. In addition, $D_h(\omega)$ is the hydraulic damping and K_h is the buoyant stiffness. On the right-hand side of (2.1), f_e represents the wave excitation force and f_p is the force generated by the PTO mechanism. Under regular (sinusoidal) wave and linear PTO assumptions, f_e and f_p can be specified as

$$\begin{cases} f_e = F(\omega, H)\cos(\omega t), \\ f_p = -D_p\dot{q} - K_p q. \end{cases} \tag{2.2}$$

Here, $F(\omega, H)$ is the magnitude of f_e that depends on ω and the wave amplitude, H. Also, D_p and K_p are the equivalent PTO damping and stiffness, which can be potentially controlled to optimize the energy extraction.

2.2 Problem Formulation on Power Maximization

Based on the aforementioned model, the instantaneous power output can be characterized as follows

$$P(t) = -f_p(t)\dot{q}(t) = (D_p\dot{q}(t) + K_p q(t))\dot{q}(t). \tag{2.3}$$

However, regardless of the transient state, we are interested in the time-averaged steady-state power output

$$P^{ss}_{\text{avg}} \triangleq \frac{1}{T_p}\int_0^{T_p} P_{ss}(\tau)\,\mathrm{d}\tau, \tag{2.4}$$

where T_p is the wave period, i.e., $T_p = 2\pi/\omega$, and $P_{ss}(t)$ is the steady-state behavior of the power output $P(t)$ introduced in (2.3). As illustrated in [6], the following optimal conditions maximize P_{avg}^{ss}

$$\begin{cases} \omega = \sqrt{\frac{K_h+K_p}{M_s+M_a(\omega)}}, \\ D_p = D_h(\omega). \end{cases} \tag{2.5}$$

However, a direct tuning of the control parameters D_p and K_p according to (2.5) may not be feasible, since $M_a(\omega)$, $D_h(\omega)$, and $F(\omega, H)$ are related to the wave conditions and the geometry of the buoy in a complicated manner, and the real wave conditions vary in different time-scales [7]. Motivated by the above facts, model-free extremum-seeking control techniques can be used to deal with this problem, which we will develop more later.

For simplicity, we denote $M \triangleq M_s + M_a(\omega)$, $K \triangleq K_h + K_p$. Also, we only take $v = D_p$ to be the control variable and keep $K_p = 0$. However, our approach can be extended to the case when $v = (D_p, K_p)^T$ in a straightforward manner. Based on (2.1) and (2.2), we get

$$M\ddot{q} + (D_h + v)\dot{q} + Kq = F\cos(\omega t),$$

or equivalently, in state-space form

$$\dot{x} = \begin{bmatrix} 0 & 1 \\ -\frac{K}{M} & -\frac{D_h+v}{M} \end{bmatrix} x + \frac{F}{M}\cos(\omega t), \tag{2.6}$$

where $x = (x_1, x_2)^T = (q, \dot{q})^T \in \mathbb{R}^2$. For the sake of power-output efficiency, as discussed in [13], we constrain v to belong to a compact set, $Q = [v^{\min}, v^{\max}]$, where $v^{\min}$ and $v^{\max}$ are given beforehand and satisfy $0 \le v^{\min} < v^{\max}$. Besides, the other parameters are real and positive, in accordance with their physical interpretations.

The objective is to optimize the time-averaged steady-state power output as follows

$$\max_{v\in Q} P_{\text{avg}}^{ss}(v),$$
$$\text{s.t. } (2.6).$$

Due to the presence of the constraint set, Q, as well as the lack of explicit knowledge on the parameters, F, K, M, and D_h, we focus on the approach of sampled-data ES, which iteratively updates the control parameters, based on the feeding of the sampled outputs, to minimize or maximize the steady-state output map of the plant. This leads the problem of how to realize the interconnection of the numerical scheme and dynamic system, so that the stability of the coupled system is guaranteed while maximizing the desired performance function. We address this issue in the rest of the contents.

Chapter 2, in full, has been submitted for publication of the material as it may appear in proceedings of the 2014 American Control Conference, Portland, OR, June 2014, Tianjia Chen, Hamed Foroush and Sonia Martinez. The thesis author was the primary investigator and author of this paper.

Chapter 3

Sampled-Data Extremum-Seeking: Theory

In this chapter, we present theoretical results on constrained sampled-data ES for a general class of systems. The contents are kept abstract and have been inspired from [11]. Nonetheless, they have been adapted for the class of discrete-time systems with constrained control inputs that we consider here.

3.1 General Setting

We consider a class of discrete-time nonlinear systems described as

$$\Sigma : \begin{cases} x_{j+1} = f(x_j, v_j), \\ y_j = h(x_j, v_j), \end{cases} \quad j \in \mathbb{N},$$

where $x \in \mathbb{R}^n$ is the state vector, $v \in Q \subset \mathbb{R}^d$ is the input vector in a compact set Q, and $y \in \mathbb{R}$ is the output. Here, the mappings f and h are continuous. We shall study the stability behavior of Σ when interconnected with a numerical optimization algorithm of the form

$$\mathcal{O} : v^{k+1} = v^k + s(v^k), \ \ \forall k \in \mathbb{N}, \tag{3.1}$$

where $s(v^k)$ is the so-called search vector at the k^{th} iteration. We notice the use of different indices for Σ and $\mathcal{O}$ to indicate that the time-steps for both systems need not be necessarily the same. To be precise, subscripts j's characterize the time-sequence $\{t_j\}$, where $t_j = jT_\Sigma$; while superscripts k's characterize the time-sequence $\{t^k\}$, where $t^k = kT_\mathcal{O}$, with $T_\mathcal{O} = nT_\Sigma$ for some $n \in \mathbb{N}$.

Intuitively, the system interconnection $\Sigma - \mathcal{O}$ is performed when feeding the plant Σ a proper control input v, generated by controller $\mathcal{O}$, which aims to optimize some cost function. In the context of sampled-data ES, the stability of the interconnection $\Sigma - \mathcal{O}$ is usually characterized by $T_\mathcal{O}$. In what follows, this point is formalized in technical words.

We assume that there exists a continuous *fixed-point map* $l : Q \to \mathbb{R}^n$ such that $f(x, v) = x$ if and only if $x = l(v)$. Using l we define the new state variable $z \triangleq x - l(v)$. Thereby, a state transformation on Σ is performed for a fixed input $v_j \equiv v, \forall j \in \mathbb{N}$, leading to

$$\Sigma : \begin{cases} z_{j+1} = f(z_j + l(v), v) - l(v), \\ y_j = h(z_j + l(v), v). \end{cases} \quad j \in \mathbb{N}. \tag{3.2}$$

Moreover, we define the *Reference-to-Output* (RO) map, $J : Q \to \mathbb{R}$, as $J(v) = h(l(v), v)$. Once Σ and $\mathcal{O}$ are interconnected, we can regard the effect of Σ on $\mathcal{O}$ as a perturbation on $\mathcal{O}$'s ideal evolution described in (3.1). The perturbed numerical optimization algorithm evolves according to

$$\mathcal{O}_p : \begin{cases} v^{k+1} = v^k + s_p(v^k, z^k), \ \ \forall k \in \mathbb{N}, \\ v_j = v^k, \ \ \forall j \in \mathbb{N} : t_j \in [t^{k-1}, t^k), \end{cases} \tag{3.3}$$

where $s_p(v, z)$ is the perturbed search vector satisfying $v + s_p(v, z) \in Q$. Let us define also z^k be the transient error for the k^{th} iteration as

$$z^k \triangleq x^k - l(v^k), \tag{3.4}$$

where $x^k = x(t^k)$.

In what follows, we shall state several different assumptions required for later analysis.

Assumption 3.1.1. *(Lyapunov function for Σ): For every fixed $v \in \mathbb{R}^d$, the dynamic system Σ described in* (3.2) *is exponentially stable. That is, there exists a radially unbounded C^1 function, $V_\Sigma : \mathbb{R}^n \to \mathbb{R}_{\geq 0}$, such that*

(a) $V_\Sigma(z)$ *is positive definite,*

(b) there exists a real number $\gamma > 0$ such that

$$V_\Sigma(z_{j+1}) = V_\Sigma(f(z_j + l(v), v) - l(v)) \leq e^{-\gamma T_\Sigma} V_\Sigma(z_j),$$

$\forall z_j \in \mathbb{R}^n$, $\forall v \in Q$, *where T_Σ denotes the time-step of Σ, as stated previously.*

Remark 3.1.2. *Due to the continuity of the composition, $J(v) = h(l(v), v)$, with respect to v and the compactness property of Q, there exists a $v^* \in Q$ such that $\forall v \in Q$, $J(v) \geq J(v^*)$. Moreover, the next assumption guarantees that numerical optimization algorithm $\mathcal{O}$ converges to this v^*.*

Assumption 3.1.3. *(Lyapunov function for $\mathcal{O}$): The numerical optimization algorithm $\mathcal{O}$ converges to v^*, a minimizer of $J(v)$. More precisely, there exists a C^1 function $V_\mathcal{O} : Q \to \mathbb{R}_{\geq 0}$ with the following properties:*

(a) $V_\mathcal{O}(v)$ *be positive definite,*

(b) $\nabla V_\mathcal{O}(v)^T s(v) < 0$, $\forall v \in Q \backslash \{v^*\}$, *and* $\nabla V_\mathcal{O}(v^*)^T s(v^*) = 0$,

(c) there exist a real number $\kappa_s > 0$ such that $|s(v)|^2 \leq -\kappa_s \nabla V_\mathcal{O}(v)^T s(v)$, $\forall v \in Q$,

(d) $\nabla V_\mathcal{O}(v)$ *be Lipschitz on Q, with Lipschitz constant, $L_{\nabla V_\mathcal{O}}$.*

Assumption 3.1.4. *(Additive perturbation to the search vector): There exists a continuous function, $p : \mathbb{R}^n \to \mathbb{R}^d$, such that $s_p(v, z) = s(v) + p(z)$, $\forall v \in Q$, $\forall z \in \mathbb{R}^n$.*

Remark 3.1.5. *(Expansion of the perturbation term): The term, $p(v)$, stated in the previous assumption, can be always represented as the addition of its vanishing and nonvanishing components as in the following form:*

$$p(z) = p_v(z) + p_0,$$

where $p_v(z) \triangleq p(z) - p(0)$ and $p_0 \triangleq p(0)$.

Assumption 3.1.6. *(Growth of the vanishing perturbation): There exists a real number, $\kappa_\Sigma > 0$, such that $\kappa_\Sigma V_\Sigma(z) \geq |p_v(z)|^2$, $\forall z \in \mathbb{R}^n$.*

Assumption 3.1.7. *(Lipschitz property of l): The fixed-point map $l(v)$ is Lipschitz on Q, with Lipschitz constant L_l.*

We would like to note that the assumptions mentioned above are along the lines of the ones stated in [11]. Moreover, in this adapted framework, Assumption 3.1 in [11] is relaxed, since it does not hold for the gradient-projection algorithms which are commonly used in constrained optimization and also will be involved in our particular WEC problem.

3.2 Main Theoretical Results

In this section, we present two results wherein we discuss under which conditions, the $\Sigma - \mathcal{O}$ interconnection obeys a semiglobal practical stability property.

Definition 3.2.1. *The point $(0^T, (v^*)^T)^T$ is said to be* semiglobally practically asymptotically stable *for the closed-loop system $\Sigma - \mathcal{O}$ if:*

1) *There exist two compact subsets of $\mathbb{R}^n \times Q$, i.e., P and W, with $P \subset W$, both containing $(0^T, (v^*)^T)^T$, and both being positively invariant with respect to $\Sigma - \mathcal{O}$. Furthermore, each trajectory of $\Sigma - \mathcal{O}$ starting in $W \backslash P$ must enter P in finitely-many iterations,*

2) *$\Sigma - \mathcal{O}$ is parameterized by a set of tunable variables that can be adjusted to render W arbitrarily large, and P, arbitrarily small.*

Lemma 3.2.2. *(Leibniz integral rule [11]): Given a differentiable function, $f : \mathbb{R}^n \to \mathbb{R}$, and $a, b \in \mathbb{R}^n$, we have*

$$f(a+b) = f(a) + \int_0^1 \nabla f(a + \tau b)^T b \, \mathrm{d}\tau. \tag{3.5}$$

Proof. Let $g(\tau) = a + \tau b$. By the chain rule of differentiation, we have

$$\frac{\mathrm{d}}{\mathrm{d}\tau} f(g(\tau)) = \nabla f(a + \tau b)^T b.$$

Then by Leibniz integral rule,

$$\int_0^1 \frac{\mathrm{d}}{\mathrm{d}\tau} f(a + \tau b) \mathrm{d}\tau = f(a + b) - f(a),$$

whereby equation (3.5) follows readily. $\square$

Lemma 3.2.3. *(Growth of the Lyapunov function for Σ): Let $\Delta V_\Sigma^k = V_\Sigma(z^{k+1}) - V_\Sigma(z^k)$, with z^k as in* (3.4)*, and recall $T_\mathcal{O} = nT_\Sigma$ for some $n \in \mathbb{N}$. Under Assumption 3.1.1 on the Lyapunov function of Σ and Assumption 3.1.7 on the Lipschitz properties of l, the following holds:*

$$\begin{aligned} \Delta V_\Sigma^k \leq & -(1 - e^{-\gamma T_\mathcal{O}}) V_\Sigma(z^k) + e^{-\gamma T_\mathcal{O}} |s_p(v^k, z^k)|^2 \\ & + \frac{1}{4} e^{-\gamma T_\mathcal{O}} (L_{V_\Sigma} L_l)^2, \end{aligned} \tag{3.6}$$

for all $((z^k)^T, (v^k)^T)^T \in \Omega_z \times Q$, where $\Omega_z \subset \mathbb{R}^n$ is an arbitrarily large and compact set that contains the origin, and L_{V_Σ} is the Lipschitz constant for $V_\Sigma(z)$ on some compact set $S \supset \Omega_z$.

Proof. By Assumption 3.1.1, we get

$$\begin{aligned} V_\Sigma(z^{k+1}) &= V_\Sigma(x^{k+1} - l(v^{k+1})) \\ &\leq e^{-\gamma T_\mathcal{O}} V_\Sigma(x^k - l(v^{k+1})) \\ &= e^{-\gamma T_\mathcal{O}} V_\Sigma(x^k - l(v^k) + l(v^k) - l(v^{k+1})), \end{aligned}$$

we then recall $z^k = x^k - l(v^k)$, where then adding and subtracting $e^{-\gamma T_\mathcal{O}} V_\Sigma(z^k)$ on the right-hand side, bestows

$$\begin{aligned} V_\Sigma(z^{k+1}) \leq & e^{-\gamma T_\mathcal{O}} V_\Sigma(z^k + l(v^k) - l(v^{k+1})) - e^{-\gamma T_\mathcal{O}} V_\Sigma(z^k) \\ & + e^{-\gamma T_\mathcal{O}} V_\Sigma(z^k). \end{aligned}$$

From the statement of this lemma, we know $z^k \in \Omega_z \subset \mathbb{R}^n$ where Ω_z is compact. Also, we know $v^k \in Q, v^{k+1} \in Q$ where Q is also compact. Let us then define the following set:

$$S = \{z \in \mathbb{R}^n : z = \zeta + l(v^k) - l(v^{k+1}), \zeta \in \Omega_z, \\ v^k \in Q, v^{k+1} \in Q\},$$

where we note that $S \supset \Omega_z$ and that S is compact—by recalling Assumption 3.1.7 on $l(v)$ be Lipschitz on Q. Moreover based on Assumption 3.1.1(a), we recall $V_\Sigma(z)$ is C^1, which infers that it is locally Lipschitz on any compact set. Let then L_{V_Σ} be its Lipschitz constant on the compact set S, where then by recalling Assumption 3.1.1(b) and using the Lipschitz property of $V_\Sigma(z)$ and $l(v)$, for all $z^k \in \Omega_z$, we obtain

$$\begin{aligned} V_\Sigma(z^{k+1}) &\leq e^{-\gamma T_\mathcal{O}} L_{V_\Sigma} |l(v^k) - l(v^{k+1})| + e^{-\gamma T_\mathcal{O}} V_\Sigma(z^k) \\ &\leq e^{-\gamma T_\mathcal{O}} L_{V_\Sigma} L_l |v^{k+1} - v^k| + e^{-\gamma T_\mathcal{O}} V_\Sigma(z^k). \end{aligned}$$

We then, by (3.3), notice that $v^{k+1} - v^k = s_p(v^k, z^k)$ where then by applying Young's inequality $ab \leq \frac{\epsilon}{2} a^2 + \frac{1}{2\epsilon} b^2$ with $\epsilon = 2$ on the term, $L_{V_\Sigma} L_l |s_p(v^k, z^k)|$, we derive

$$\begin{aligned} V_\Sigma(z^{k+1}) &\leq e^{-\gamma T_\mathcal{O}} L_{V_\Sigma} L_l |s_p(v^k, z^k)| + e^{-\gamma T_\mathcal{O}} V_\Sigma(z^k) \\ &\leq e^{-\gamma T_\mathcal{O}} |s_p(v^k, z^k)|^2 + \frac{1}{4} e^{-\gamma T_\mathcal{O}} (L_{V_\Sigma} L_l)^2 + e^{-\gamma T_\mathcal{O}} V_\Sigma(z^k). \end{aligned}$$

Finally, subtracting $V_\Sigma(z^k)$ from both sides gives the required form as in (3.6), and thus the proof is complete. □

We state next two theorems providing sufficient conditions to guarantee the desired stability properties for the closed-loop system $\Sigma - \mathcal{O}$ at $(0^T, v^{*T})^T$.

Theorem 3.2.4. *(Growth of the composite Lyapunvo function): Consider the composite Lyapunov function $V(z, v) = V_\Sigma(z) + V_\mathcal{O}(v)$ and let Assumptions 3.1.1 and 3.1.3 on the Lyapunov functions V_Σ and $V_\mathcal{O}$, Assumptions 3.1.7 on the Lipschitz property of l, and Assumptions 3.1.4 and 3.1.6 on the properties of the perturbation to the search vector, hold. Then, there exists a neighborhood $\Omega_0 \times Q$ of $(0^T, (v^*)^T)^T$, where $\Omega_0 \subset \mathbb{R}^n$ which can be made arbitrarily large, and positive real numbers, κ_s^*, κ_Σ^* and T^*, such that* *if* $\kappa_s < \kappa_s^*$*,* $\kappa_\Sigma < \kappa_\Sigma^*$*,* $T_\mathcal{O} > T^*$ *and* $((z^0)^T, (v^0)^T)^T \in \Omega_0 \times Q$*, then* $V(z^k, v^k)$ *decreases along the trajectories of the system* $\Sigma - \mathcal{O}$ *according to*

$$\Delta V^k \leq -C_\Sigma V_\Sigma(z^k) + C_\mathcal{O} \nabla V_\mathcal{O}^T(v^k) s(v^k) + \bar{C},$$

where $\Delta V^k \triangleq V(z^{k+1}, v^{k+1}) - V(z^k, v^k)$*. Also,* C_Σ*,* $C_\mathcal{O}$ *and* $\bar{C}$ *are positive real numbers and given by*

$$\begin{aligned}
C_\Sigma &= 1 - e^{-\gamma T_\mathcal{O}} - \kappa_\Sigma(4e^{-\gamma T_\mathcal{O}} + 2L_{\nabla V_\mathcal{O}} + \frac{1}{\delta}), \\
C_\mathcal{O} &= 1 - \kappa_s(2e^{-\gamma T_\mathcal{O}} + L_{\nabla V_\mathcal{O}}), \\
\bar{C} &= (4e^{-\gamma T_\mathcal{O}} + 2L_{\nabla V_\mathcal{O}} + \frac{1}{\delta})|p_0|^2 \\
&\quad + \frac{1}{4}e^{-\gamma T_\mathcal{O}}(L_{V_\Sigma} L_l)^2 + \frac{\delta}{2}\sup_{v \in Q}|\nabla V_\mathcal{O}(v)|^2,
\end{aligned}$$

where δ *is some positive constant.*

Proof. Under the evolution of $\Sigma - \mathcal{O}$, we have

$$\Delta V^k = V(z^{k+1}, v^{k+1}) - V(z^k, v^k) = \Delta V_\Sigma^k + \Delta V_\mathcal{O}^k,$$

where ΔV_Σ^k is as defined in Lemma 3.2.3 and $\Delta V_\mathcal{O}^k = V_\mathcal{O}(v^k + s_p(v^k, z^k)) - V_\mathcal{O}(v^k)$. From Lemma 3.2.2, we have

$$\begin{aligned}
V_\mathcal{O}(v^k + s_p(v^k, z^k)) &= V_\mathcal{O}(v^k) + \nabla V_\mathcal{O}(v^k)^T s_p(v^k, z^k) \\
&+ \int_0^1 (\nabla V_\mathcal{O}(v^k + \tau s_p(v^k, z^k)) - \nabla V_\mathcal{O}(v^k))^T s_p(v^k, z^k)\, \mathrm{d}\tau.
\end{aligned}$$

We apply the Lipschitz property of $\nabla V_\mathcal{O}$ with Lipschitz constant $L_{\nabla V_\mathcal{O}}$ on the integrand, which obtains

$$\Delta V_\mathcal{O}^k \leq \nabla V_\mathcal{O}(v^k)^T s_p(v^k, z^k) + \frac{1}{2} L_{\nabla V_\mathcal{O}} |s_p(v^k, z^k)|^2.$$

This latter inequality, together with (3.6), leads to

$$\begin{aligned}
\Delta V^k \leq &- (1 - e^{-\gamma T_\mathcal{O}})V_\Sigma + e^{-\gamma T_\mathcal{O}}|s_p|^2 + \frac{1}{4}e^{-\gamma T_\mathcal{O}}(L_{V_\Sigma} L_l)^2 \\
&+ \nabla V_\mathcal{O}^T s_p + \frac{1}{2} L_{\nabla V\mathcal{O}} |s_p|^2,
\end{aligned}$$

where we drop all the arguments for notational simplicity. We then recall from Assumption 3.1.4 that $s_p = s + p$, which implies

$$|s_p|^2 = |s|^2 + 2s^T p + |p|^2.$$

By the Cauchy-Schwarz inequality, it holds that $s^T p \leq |s||p|$ and $\nabla V_{\mathcal{O}}^T p \leq |\nabla V_{\mathcal{O}}||p|$. Therefore, we obtain

$$\begin{aligned}
\Delta V^k \leq & -(1 - e^{-\gamma T_{\mathcal{O}}})V_\Sigma \\
& + (e^{-\gamma T_{\mathcal{O}}} + \frac{1}{2}L_{\nabla V_{\mathcal{O}}})(|s|^2 + 2|s||p| + |p|^2) \\
& + \frac{1}{4}e^{-\gamma T_{\mathcal{O}}}(L_{V_\Sigma}L_l)^2 + \nabla V_{\mathcal{O}}^T s + |\nabla V_{\mathcal{O}}||p|.
\end{aligned}$$

By Young's inequality, we have that

$$\begin{aligned}
|s||p| &\leq \frac{1}{2}|s|^2 + \frac{1}{2}|p|^2, \\
|\nabla V_{\mathcal{O}}||p| &\leq \frac{\delta}{2}|\nabla V_{\mathcal{O}}|^2 + \frac{1}{2\delta}|p|^2,
\end{aligned}$$

where $\delta > 0$ is some parameter we can specify. Using the above inequalities for a generic δ, we obtain

$$\begin{aligned}
\Delta V^k \leq & -(1 - e^{-\gamma T_{\mathcal{O}}})V_\Sigma + (2e^{-\gamma T_{\mathcal{O}}} + L_{\nabla V_{\mathcal{O}}})|s|^2 \\
& + (2e^{-\gamma T_{\mathcal{O}}} + L_{\nabla V_{\mathcal{O}}} + \frac{1}{2\delta})|p|^2 \\
& + \frac{1}{4}e^{-\gamma T_{\mathcal{O}}}(L_{V_\Sigma}L_l)^2 + \nabla V_{\mathcal{O}}^T s + \frac{\delta}{2}|\nabla V_{\mathcal{O}}|^2.
\end{aligned}$$

Recall that $p(z) = p_v(z) + p_0$, which implies $|p|^2 \leq 2|p_v|^2 + 2|p_0|^2$, and Assumptions 3.1.3(c) and 3.1.6, which imply $|s|^2 \leq -\kappa_s \nabla V_{\mathcal{O}}^T s$ and $|p_v|^2 \leq \kappa_\Sigma V_\Sigma$, respectively. Thus, we can further upper bound ΔV^k as

$$\begin{aligned}
\Delta V^k \leq & (-(1 - e^{-\gamma T_{\mathcal{O}}}) + \kappa_\Sigma(4e^{-\gamma T_{\mathcal{O}}} + 2L_{\nabla V_{\mathcal{O}}} + \frac{1}{\delta}))V_\Sigma \\
& + (1 - \kappa_s(2e^{-\gamma T_{\mathcal{O}}} + L_{\nabla V_{\mathcal{O}}}))\nabla V_{\mathcal{O}}^T s \\
& + (4e^{-\gamma T_{\mathcal{O}}} + 2L_{\nabla V_{\mathcal{O}}} + \frac{1}{\delta}))|p_0|^2 \\
& + \frac{1}{4}e^{-\gamma T_{\mathcal{O}}}(L_{V_\Sigma}L_l)^2 + \frac{\delta}{2}|\nabla V_{\mathcal{O}}|^2.
\end{aligned}$$

Let us denote

$$C_{\Sigma} = 1 - e^{-\gamma T_{\mathcal{O}}} - \kappa_{\Sigma}(4e^{-\gamma T_{\mathcal{O}}} + 2L_{\nabla V_{\mathcal{O}}} + \frac{1}{\delta}),$$
$$C_{\mathcal{O}} = 1 - \kappa_s(2e^{-\gamma T_{\mathcal{O}}} + L_{\nabla V_{\mathcal{O}}}),$$

and

$$C =(4e^{-\gamma T_{\mathcal{O}}} + 2L_{\nabla V_{\mathcal{O}}} + \frac{1}{\delta})|p_0|^2 + \frac{1}{4}e^{-\gamma T_{\mathcal{O}}}(L_{V_{\Sigma}}L_l)^2 + \frac{\delta}{2}|\nabla V_{\mathcal{O}}|^2.$$

We obtain the desired upper bound for ΔV^k as

$$\Delta V^k \leq -C_{\Sigma}V_{\Sigma} + C_{\mathcal{O}}\nabla V_{\mathcal{O}}^T s + \bar{C},$$

where $\bar{C} > 0$ is given by

$$\bar{C} =(4e^{-\gamma T_{\mathcal{O}}} + 2L_{\nabla V_{\mathcal{O}}} + \frac{1}{\delta})|p_0|^2 + \frac{1}{4}e^{-\gamma T_{\mathcal{O}}}(L_{V_{\Sigma}}L_l)^2 + \frac{\delta}{2}\sup_{v\in Q}|\nabla V_{\mathcal{O}}(v)|^2.$$

Observe that $C_{\mathcal{O}}$ can always be rendered positive for a $\kappa_s < \kappa_s^*$ where

$$\kappa_s^* = \frac{1}{2 + L_{\nabla V_{\mathcal{O}}}}.$$

Regarding C_{Σ}, we can fix a chosen $T^* > 0$ and then, $\epsilon^* \triangleq 1 - e^{-\gamma T^*}$ satisfies $0 < \epsilon^* < 1$. Moreover, note that it is possible to choose a $\kappa_{\Sigma} > 0$ small enough so that

$$\kappa_{\Sigma}(4e^{-\gamma T_{\mathcal{O}}} + 2L_{\nabla V_{\mathcal{O}}} + \frac{1}{\delta}) < \epsilon^*,$$

for any fixed parameter δ and any $T_{\mathcal{O}} > 0$. Indeed, such a choice of κ_{Σ} can be characterized by $\kappa_{\Sigma} < \kappa_{\Sigma}^*$, where

$$\kappa_{\Sigma}^* = \frac{\epsilon^*}{4 + 2L_{\nabla V_{\mathcal{O}}} + \frac{1}{\delta}} \leq \frac{\epsilon^*}{4e^{-\gamma T_{\mathcal{O}}} + 2L_{\nabla V_{\mathcal{O}}} + \frac{1}{\delta}}.$$

Thus, along with the condition $T_{\mathcal{O}} > T^*$, C_{Σ} can be ensured to be positive.

We note that the prerequisite for the above arguments is that $((z^k)^T, (v^k)^T)^T \in \Omega_z \times Q$ in Lemma 3.2.3 holds. Therefore, the set Ω_0 in the theorem statement can be chosen to be inside of Ω_z which can be made arbitrarily large.

$\square$

We note that in the case of forward-Euler gradient estimation, where $p_0 = \mu_s \bar{p}_0$ and μ_s is the step-size in the Euler method, $\bar{C}$ can be tuned to be arbitrarily small by taking large enough $T_{\mathcal{O}}$ and small enough μ_s depending on the specified δ. Based on the previous theorem and Definition 3.2.1, we are now ready to characterize the semiglobal practical asymptotic stability property of the $\Sigma - \mathcal{O}$ system in the following theorem.

Theorem 3.2.5. *(Stability of the interconnected $\Sigma - \mathcal{O}$): Assume that the conditions of Theorem 3.2.4, on the growth of the composite Lyapunov function, are satisfied with $\kappa_s < \kappa_s^*$, $\kappa_\Sigma < \kappa_\Sigma^*$ and $T_{\mathcal{O}} > T^*$. Furthermore, assume that the nonvanishing perturbation p_0 is parametrized by a tunable variable μ_s as $p_0 = \mu_s \bar{p}_0$. Then, the system $\Sigma - \mathcal{O}$ is semiglobally practically asymptotically stable at $(0^T, (v^*)^T)^T$.*

Proof. The proof mimics the approach discussed in the proof of Theorem 3.2 in [11]. Consider $w = (z^T, v^T)^T \in \mathbb{R}^n \times Q$ and let $w^* = (0^T, v^{*T})^T$. Define the set

$$Z = \{w \in \mathbb{R}^n \times Q : C_\Sigma V_\Sigma(z) - C_{\mathcal{O}} \nabla V_{\mathcal{O}}(v)^T s(v) \leq \bar{C}\}.$$

Note that on Z, the sequence $\{V(w^k)\}_{k \geq 0}$ generated by the evolution of $\Sigma - \mathcal{O}$ is no longer guaranteed to decrease. By Assumptions 3.1.1 and 3.1.3, the function $F : w \mapsto C_\Sigma V_\Sigma(z) - C_{\mathcal{O}} \nabla V_{\mathcal{O}}(v)^T s(v)$ is continuous and positive definite. Consequently, Z is compact for a sufficiently small $\bar{C} > 0$. Moreover, since the parameter,

$$\begin{aligned}\bar{C} =& (4e^{-\gamma T_{\mathcal{O}}} + 2L_{\nabla V_{\mathcal{O}}} + \frac{1}{\delta})|p_0|^2 \\ &+ \frac{1}{4} e^{-\gamma T_{\mathcal{O}}} (L_{V_\Sigma} L_l)^2 + \frac{\delta}{2} \sup_{v \in Q} |\nabla V_{\mathcal{O}}(v)|^2.\end{aligned}$$

can be made arbitrarily small for small μ_s and large $T_{\mathcal{O}}$, the set Z itself can be made arbitrarily small by the continuity of F.

We may now construct the required set P discussed in Definition 3.2.1. By the compactness of Z and the continuity of V, there exists a number $\beta = \max\{V(w) : w \in Z\}$; then, $\Omega_\beta = \{w \in \mathbb{R}^n \times Q : V(w) \leq \beta\}$ is the smallest sublevel set of V strictly containing Z. We claim that the set

$$\Omega_{\beta + \bar{C}} \triangleq \{w \in \mathbb{R}^n \times Q : V(w) \leq \beta + \bar{C}\},$$

is positively invariant with respect to $\Sigma - \mathcal{O}$. Since Ω_β is the smallest sublevel set of V containing Z, it is clear that $\Omega_{\beta+\bar{C}}$ is the smallest positively invariant set containing Z.

Next, let ϵ be a positive, arbitrarily small, real number and consider the larger sublevel set

$$P \triangleq \{w \in \mathbb{R}^n \times Q : V(w) \leq \beta + \bar{C} + \epsilon\},$$

which is compact since both V_Σ is positive definite and radially unbounded and $V_\mathcal{O}$ is positive definite and Q is compact. We note that by the construction of P from Z, and the fact that Z can be made arbitrarily small via $T_\mathcal{O}$ and μ_s, P can likewise be made arbitrarily small.

Choose any W according to Theorem 3.2.4, large enough to strictly contain P. Such a choice is always possible by the radial unboundedness of V_Σ and the compactness of Q. In the following, we show that all trajectories initiated inside $W \backslash P$ enter P in finitely-many iterations. Since W is compact, there exists a number

$$a = \min\{-\Delta V(w) : w \in W \backslash P\}.$$

Suppose that $\Sigma - \mathcal{O}$ is initialized at $w^0 \in W \backslash P$. Then $V(w^{k+1}) < V(w^k) - a$ and therefore $V(w^k) < V(w^0) - ka$, which implies that $w^k \in P$ for all $k > K$, where

$$K = \lceil \frac{V(w^0) - \beta - \bar{C} - \epsilon}{a} \rceil.$$

Since w^0 is arbitrary, it remains true that all trajectories initiated inside $W \backslash P$ enter P in finitely-many iterations, and Definition 3.2.1 is satisfied, and thus the proof is complete. $\square$

Chapter 3, in part, has been submitted for publication of the material as it may appear in proceedings of the 2014 American Control Conference, Portland, OR, June 2014, Tianjia Chen, Hamed Foroush and Sonia Martinez. The thesis author was the primary investigator and author of this paper.

Chapter 4

Sampled-Data Extremum-Seeking: Application

In this chapter, we first discuss the steady-state behavior of the buoy dynamics, where we shall also introduce the output and reference-to-output maps. We then present our NES algorithm, which is followed by applying the sampled-data ES theory to analyze the stability of this algorithm.

4.1 Steady-State Behavior and Output Maps

We first recall that

$$M\ddot{q} + (D_h + v)\dot{q} + Kq = F\cos(\omega t), \tag{4.1}$$

and let $u(t) = F\cos(\omega t)$. Applying the Laplace transform on this equation we get

$$s^2 MX(s) + s(D_h + v)X(s) + KX(s) = U(s),$$

wherein $X(s) \triangleq \mathcal{L}_t\{q(t)\}(s)$, $U(s) \triangleq \mathcal{L}_t\{u(t)\}(s)$. Accordingly, we can obtain the following transfer function

$$G(s) \triangleq \frac{X(s)}{U(s)} = \frac{1}{Ms^2 + (D_h + v)s + K}.$$

Recall that the steady-state response to sinusoidal input signal $u(t) = F\cos(\omega t)$ is

$$q_{ss}(t) = FX_m \cos(\omega t + \phi), \tag{4.2}$$

where X_m and ϕ represent the complex modulus and argument of $G(i\omega)$, respectively, with $i = \sqrt{-1}$. Thus, X_m can be computed as

$$X_m = |G(i\omega)| = \frac{1}{\sqrt{(K - M\omega^2)^2 + (D_h + v)^2\omega^2}}. \tag{4.3}$$

It can also be verified that

$$\dot{q}_{ss}(t) = \omega F X_m(-\sin(\omega t + \phi)). \tag{4.4}$$

Based on this, we are able to find the relation between P^{ss}_{avg}, as defined in Chapter 2, and the control variable v.

Lemma 4.1.1. *(Steady-state averaged power): Consider system dynamics* (4.1)*, then* P^{ss}_{avg}*, as defined by*

$$P^{ss}_{\text{avg}} \triangleq \frac{1}{T_p}\int_0^{T_p} P_{ss}(\tau)\,\mathrm{d}\tau, \tag{4.5}$$

satisfies

$$P^{ss}_{\text{avg}}(v) = \frac{1}{2}\frac{\omega^2 F^2 v}{(K - M\omega^2)^2 + (D_h + v)^2\omega^2}. \tag{4.6}$$

Proof. First, we recall from Chapter 2 that

$$P(t) = -f_p(t)\dot{q}(t) = (D_p\dot{q}(t) + K_p q(t))\dot{q}(t),$$

whereby we note that $P_{ss}(t)$, the steady-state behavior of power output $P(t)$ can be further derived by $P_{ss}(t) = (D_p\dot{q}_{ss}(t) + K_p q_{ss}(t))\dot{q}_{ss}(t)$. By replacing $q_{ss}(t)$ and $\dot{q}_{ss}(t)$ with equations (4.2) and (4.4), we obtain

$$\begin{aligned}
P^{ss}_{\text{avg}} &= \frac{1}{T_p}\int_0^{T_p} v\omega^2 F^2 X_m^2 \sin^2(\omega\tau + \phi)\,\mathrm{d}\tau \\
&\quad + \frac{1}{T_p}\int_0^{T_p} K_p\omega F^2 X_m^2(-\frac{1}{2}\sin(2\omega\tau + 2\phi))\,\mathrm{d}\tau \\
&= \frac{1}{2}v\omega^2 F^2 X_m^2,
\end{aligned}$$

where we note $v = D_p$. Finally, recalling equation (4.3), we obtain (4.6); this then completes the proof. $\square$

Next, we consider the following output map:

$$y(t) = h(x,v) = -\frac{1}{2}v(t)(\omega^2(x_1(t))^2 + (x_2(t))^2), \tag{4.7}$$

provided that the states $x = (x_1, x_2)^T = (q, \dot{q})^T$ are available by employing velocity and acceleration sensors, and that the wave frequency ω is detectable by using wave gauges or optical-fiber sensors as in [18]. The steady-state behavior of this output map is characterized in the next lemma.

Lemma 4.1.2. *(Output map): Consider the output map $y(t)$ given by* (4.7)*, and let $J(v) = \lim_{t\to\infty} y(t)|_{v \text{ is fixed}}$, then, the following holds*

$$J(v) = -P^{ss}_{\text{avg}}(v). \tag{4.8}$$

Proof. We first substitute (4.7) in $J(v)$, which can be computed recalling (4.2) and (4.4), as follows

$$J(v) = -\frac{1}{2}v(\omega^2(q_{ss}(t))^2 + (\dot{q}_{ss}(t))^2) = -\frac{1}{2}v\omega^2F^2X_m^2.$$

The result follows immediately by recalling X_m from (4.3) and comparing with $P^{ss}_{\text{avg}}(v)$ in (4.6). $\square$

Now it is clear that maximizing $P^{ss}_{\text{avg}}(v)$ is equivalent to minimizing $J(v)$. Therefore, by (4.7) and recalling

$$\dot{x} = \begin{bmatrix} 0 & 1 \\ -\frac{K}{M} & -\frac{D_h+v}{M} \end{bmatrix} x + \frac{F}{M}\cos(\omega t), \tag{4.9}$$

the system of interest is

$$\begin{cases} \dot{x} = \begin{bmatrix} 0 & 1 \\ -\frac{K}{M} & -\frac{D_h+v}{M} \end{bmatrix} x + \frac{F}{M}\cos(\omega t), \\ y = -\frac{1}{2}v(\omega^2 x_1^2 + x_2^2). \end{cases} \tag{4.10}$$

4.2 Optimization Algorithm

In order to minimize $J(v)$ stated in (4.8), here we consider a gradient-descent algorithm, which iteratively updates the control variable v as follows

$$v^{k+1} = v^k - \alpha_s \nabla J(v^k), \tag{4.11}$$

where k is the iteration index and $\alpha_s > 0$ is the fixed step-size. Note that $\nabla J(v^k)$ cannot be measured directly, so we approximate it by the forward-Euler method, that is

$$\nabla J(v^k) \approx \frac{J(v^k + \mu_s) - J(v^k)}{\mu_s}, \tag{4.12}$$

where μ_s is the step size in the Euler method. We also note that the precise value of J in (4.12) is not available because of its steady-state nature described in (4.8). Instead, we approximate it by measuring the output $y(t)$ after waiting a certain period of time, called *waiting time*, every time a new v is applied. More specifically, consider the start of the k^{th} iteration, $t^{k,0}$. At this time, we apply v^k. After waiting a period of time, at t^k, we take the measurement $y(t^k)$, right before applying $v^k + \mu_s$. Then, after waiting for another period of time, at $t^{k,1}$, we take the measurement of $y(t^{k,1})$ and update the control to be v^{k+1}. This $t^{k,1}$ then becomes the starting time instant for the next iteration, $t^{k,1} = t^{k+1,0}$. For simplicity, we set the two waiting times to be the same and equal to period T in the algorithm. Indeed, this parameter, T, plays the role of $T_{\mathcal{O}}$ introduced in Chapter 3.

We denote the above estimation of $\nabla J(v^k)$ by $\widehat{\nabla J}(v^k)$ and recall $y(t)$ from (4.7), we get

$$\widehat{\nabla J}(v^k) = \frac{h(x(t^{k,1}), v^k + \mu_s) - h(x(t^k), v^k)}{\mu_s}. \tag{4.13}$$

We recall from our problem formulation that the control variable v is constrained to $Q = [v^{\min}, v^{\max}]$. Therefore, we reformulate (4.11) as

$$v^{k+1} = \mathcal{P}_Q\{v^k - \alpha_s \nabla J(v^k)\}, \tag{4.14}$$

where the projection $\mathcal{P}_Q\{v\}$ is given by

$$\mathcal{P}_Q\{v\} = \begin{cases} v^{\min}, & \text{if } v < v^{\min}, \\ v^{\max}, & \text{if } v > v^{\max}, \\ v, & \text{otherwise}. \end{cases} \tag{4.15}$$

We assume, without loss of generality, that $\mathcal{P}_Q\{v^k + \mu_s\} = v^k + \mu_s$ holds, otherwise the following analysis can be applied with $\tilde{Q} = [v^{\min} + \mu_s, v^{\max} - \mu_s] \subseteq Q$. We further assume that the dither satisfies $\mu_s < \frac{v^{\max} - v^{\min}}{2}$, to guarantee $\tilde{Q} \neq \emptyset$.

Algorithm 1 Numerical Extremum-Seeking (NES)

given T, μ_s, α_s, $v^{\min}$, $v^{\max}$ and v_0
initialize $\tau \leftarrow 0$, $v \leftarrow v_0$
loop
  $\tau \leftarrow \tau + \Delta t$
  if $\tau > T$ and $\tau \leq T + \Delta t$ **then**
    $y_{\text{ref}} \leftarrow y(t)$,
    $v_{\text{ref}} \leftarrow v$,
    $v \leftarrow v_{\text{ref}} + \mu_s$
  else if $\tau > 2T$ and $\tau \leq 2T + \Delta t$ **then**
    $\nabla J \leftarrow \frac{y(t) - y_{\text{ref}}}{v - v_{\text{ref}}}$
    $v_{\text{ref}} \leftarrow v_{\text{ref}} - \alpha_s \nabla J$
    if $v_{\text{ref}} \geq v^{\min}$ and $v_{\text{ref}} \leq v^{\max}$ **then**
      $v \leftarrow v_{\text{ref}}$
    else if $v_{\text{ref}} < v^{\min}$ **then**
      $v \leftarrow v^{\min}$
    else if $v_{\text{ref}} > v^{\max}$ **then**
      $v \leftarrow v^{\max}$
    end if
    $\tau \leftarrow 0$
  end if
end loop

A pseudo-code for the proposed algorithm is provided in Algorithm 1, which we shall refer to as the NES algorithm. There, we use Δt to denote the algorithm's time step-size, which can be arbitrarily small and satisfies $\Delta t < T$. Also, $\tau \in \mathbb{R}_{\geq 0}$ is the algorithm's time-counter whose step-size is Δt, and which is reset after passing every $2T$ time-interval.

4.3 Stability Analysis

Recalling the steady-state response (4.2) and (4.4), there exists a limit cycle for system (4.9) for a fixed v. That is,

$$\frac{x_1^2}{F^2 X_m(v)^2} + \frac{x_2^2}{\omega^2 F^2 X_m(v)^2} = 1, \tag{4.16}$$

where $X_m(v)$ is given by (4.3). The stability of this limit cycle can be studied through a Poincaré map.

Consider (4.1), and denote by $\mu(v) \triangleq (D+v)/(2M)$, $\omega_0^2 \triangleq K/M$, and $\eta \triangleq F/M$. A more standard form of this equation can be obtained as

$$\ddot{q} + 2\mu(v)\dot{q} + \omega_0^2 q = \eta \cos(\omega t). \tag{4.17}$$

In this section, we consider the system to be underdamped, i.e., $0 < \mu(v) < \omega_0$ holds, which is generally the case for the point absorber [2]. For the other cases, similar analysis can be done in a straightforward way.

Lemma 4.3.1. *(Poincaré map for* (4.17)*; see [16]): Consider the system in* (4.17)*. We denote $\xi \triangleq \sqrt{\omega_0^2 - \mu(v)^2}$ and recall $T_p = 2\pi/\omega$. Then, a Poincaré map $\mathbb{P}$ takes the form as*

$$\mathbb{P}\begin{pmatrix} q(0) \\ \dot{q}(0) \end{pmatrix} = \begin{pmatrix} p_1(q(0), \dot{q}(0)) \\ p_2(q(0), \dot{q}(0)) \end{pmatrix}, \tag{4.18}$$

with

$$\begin{aligned} p_1 &= c_1 e^{-\mu(v)T_p} \cos(\xi T_p) + c_2 e^{-\mu(v)T_p} \sin(\xi T_p) + \alpha, \\ p_2 &= e^{-\mu(v)T_p} \cos(\xi T_p)(-c_1\mu(v) + c_2\xi) \\ &\quad - e^{-\mu(v)T_p} \sin(\xi T_p)(c_1\xi + \mu(v)c_2) + \omega\beta, \end{aligned}$$

where

$$\begin{aligned} c_1 &= q(0) - \alpha, \\ c_2 &= (\dot{q}(0) + \mu(v)q(0) - \mu(v)\alpha - \omega\beta)/\xi, \end{aligned} \tag{4.19}$$

and

$$\begin{aligned} \alpha &= \tfrac{\omega_0^2 - \omega^2}{4\mu(v)^2\omega^2 + (\omega_0^2 - \omega^2)^2}\eta, \\ \beta &= \tfrac{2\mu(v)\omega}{4\mu(v)^2\omega^2 + (\omega_0^2 - \omega^2)^2}\eta. \end{aligned} \tag{4.20}$$

Proof. The method for constructing Poincaré maps is well known. We include the proof for completeness of presentation. Clearly, $0 < \mu(v) < \omega_0$ should be satisfied to make sure the solution of (4.17) does not blow up. Then, the solution can be obtained as

$$\begin{aligned} q(t) = &c_1 e^{-\mu(v)t}\cos(\xi t) + c_2 e^{-\mu(v)t}\sin(\xi t) \\ &+ \alpha\cos(\omega t) + \beta\sin(\omega t), \end{aligned} \tag{4.21}$$

where the parameters α and β are as shown in (4.20), and the constants c_1 and c_2 are determined by initial condition $(q(0), \dot{q}(0))^T$ as in (4.19).

We note that the dynamics (4.17) is T_p-periodic in t and that it has one periodic solution $\alpha\cos(\omega t) + \beta\sin(\omega t)$ with period T_p. Therefore, we construct a Poincaré map by considering the intersections of orbit (4.21) with the q-$\dot{q}$ plane at times $t_j = jT_p, j \in \mathbb{N} \cup \{0\}$. Due to the T_p-periodicity of (4.17), we can obtain the Poincaré map $\mathbb{P}$ by evaluating the map from $(q(0), \dot{q}(0))^T$ to $(q(T_p), \dot{q}(T_p))^T$. Thus, by substituting $t = T_p$ into (4.21), we finally get (4.18), which then completes the proof. □

The Poincaré map (4.18), together with the output map $y = h(x, v)$ in (4.7) define the discrete-time system Σ corresponding to the previous chapter. That is,

$$\Sigma : \begin{cases} x_{j+1} = \mathbb{P}(x_j), \\ y_j = h(x_j, v). \end{cases}$$

Also, the ideal optimizer corresponding to the NES algorithm, as described in (4.14), can be represented in a generic form as follows

$$\mathcal{O}: \begin{array}{l} v^{k+1} = v^k + s(v^k), \\ s(v^k) = \mathcal{P}_Q\{v^k - \alpha_s \nabla J(v^k)\} - v^k. \end{array} \tag{4.22}$$

It can be easily verified that the fixed point for the map $\mathbb{P}$ in (4.18) is $x_\star = (\alpha, \omega\beta)^T$, where α and β depend on v as described in (4.20). Therefore, the fixed-point map for Σ becomes

$$l(v) = \begin{pmatrix} \alpha(v) \\ \omega\beta(v) \end{pmatrix}. \tag{4.23}$$

Then, the transient error can be defined as

$$z \triangleq x - l(v), \tag{4.24}$$

which can be used to transform Σ into

$$\Sigma: \begin{cases} z_{j+1} = A(v) z_j, \\ y_j = h(z_j + l(v), v), \end{cases} \tag{4.25}$$

where $A(v) = [a_{ij}] \in \mathbb{R}^{2\times 2}$ has entries

$$\begin{aligned} a_{11} &= e^{-\mu(v)T_p}(\cos(\xi T_p) + \frac{\mu(v)}{\xi}\sin(\xi T_p)), \\ a_{12} &= e^{-\mu(v)T_p}\frac{1}{\xi}\sin(\xi T_p), \\ a_{21} &= e^{-\mu(v)T_p}(-\frac{\xi^2 + \mu(v)^2}{\xi}\sin(\xi T_p)), \\ a_{22} &= e^{-\mu(v)T_p}(\cos(\xi T_p) - \frac{\mu(v)}{\xi}\sin(\xi T_p)). \end{aligned}$$

The C^1 function $l(v)$ in (4.23) on Q is Lipschitz with constant L_l, which verifies Assumption 3.1.7 on the Lipschitz property of l.

The RO map is defined as $J(v) = h(l(v), v)$, where the output map $h(x, v)$ is given in (4.7). By substituting (4.20), into (4.7), we obtain

$$J(v) = -\frac{1}{2}\frac{\omega^2 F^2 v}{(K - M\omega^2)^2 + (D_h + v)^2\omega^2}. \tag{4.26}$$

Note that since $J(v)$ is a continuous function on compact set Q, the existence of v^* is guaranteed.

For Σ in (4.25), we consider

$$V_\Sigma(z) = z^T P z + (z^T P z)^2, \tag{4.27}$$

where the matrix $P = P^T \succ 0$ is the unique solution to the discrete Lyapunov equation

$$A^T P A - P = -I, \tag{4.28}$$

with I be the identity matrix. This $V_\Sigma(z)$ satisfies Assumption 3.1.1 on the Lyapunov function V_Σ, which is shown in the following lemmas.

Lemma 4.3.2. *(Eigenvalues of P): Suppose P is the solution to the discrete Lyapunov equation* (4.28)*, then the eigenvalues of P, denoted by $\lambda(P)$, satisfy $\lambda(P) > 1$.*

Proof. First, we notice that the eigenvalues of system matrix A of (4.25) can be obtained as

$$\lambda_{1,2}(A) = e^{-\mu T_p}(\cos(\xi T_p) \pm i\sqrt{1 - \cos^2(\xi T_p)}),$$

whereby, we infer that the matrix A is nonsingular, because none of its eigenvalues is zero. Also, we recall that the matrix P is symmetric positive definite, which implies $A^T P A \succ 0$. Thus, we have $P - I = A^T P A \succ 0$, which implies $\lambda(P - I) > 0$, which in turn implies $\lambda(P) > 1$. $\square$

Lemma 4.3.3. *(V_Σ satisfies Assumption 3.1.1): The function $V_\Sigma(z) = z^T P z + (z^T P z)^2$ satisfies Assumption 3.1.1 on the desired properties for the Lyapunov function of* (4.25)*.*

Proof. Item (a) follows immediately from $P = P^T \succ 0$. To prove (b), we consider two cases:

Case (i): If $z_j = 0$, then $V_\Sigma(z_{j+1}) = V_\Sigma(z_j) = 0$, satisfying item (b) for any $\gamma > 0$.

Case (ii): If $z_j \neq 0$, then since $e^{-\gamma T_p} \in (0,1)$, for $\gamma > 0$, it is sufficient to show $V_\Sigma(z_{j+1}) < V_\Sigma(z_j)$ for every $j \in \mathbb{N} \cup \{0\}$. By (4.25) and (4.28), we derive

$$\begin{aligned} V_\Sigma(z_{j+1}) &= z_j^T A^T P A^T z_j + (z_j^T A^T P A^T z_j)^2 \\ &= z_j^T (P - I) z_j + (z_j^T (P - I) z_j)^2 \\ &= z_j^T P z_j + (z_j^T P z_j)^2 \\ &\quad - z_j^T z_j - 2(z_j^T P z_j)(z_j^T z_j) + (z_j^T z_j)^2 \\ &= V_\Sigma(z_j) + W(z_j), \end{aligned}$$

where we denote $W(z_j) \triangleq -z_j^T z_j - 2(z_j^T P z_j)(z_j^T z_j) + (z_j^T z_j)^2$. It can be seen that

$$W(z_j) \leq (1 - 2\lambda_{\min}(P))|z_j|^4 - |z_j|^2 < 0,$$

where we employ $|z_j|^2 = z_j^T z_j$ and that $1 - 2\lambda_{\min}(P) < 0$ according to Lemma 4.3.2. Thus, we conclude $V_\Sigma(z_{j+1}) < V_\Sigma(z_j)$ for all $z_j \neq 0$. □

We would also like to mention that this particular form of $V_\Sigma(z)$ is chosen to verify Assumption 3.1.6 on the vanishing perturbation, which is addressed later.

Lemma 4.3.4. *($V_\mathcal{O}$ satisfies Assumption 3.1.3): The choice of $V_\mathcal{O}(v) = J(v) - J(v^*)$, where $J(v)$ is the RO map stated in* (4.26)*, satisfies Assumption 3.1.3 on the Lyapunov function $V_\mathcal{O}$.*

Proof. We shall check each item in Assumption 3.1.3 as follows.

(a) $V_\mathcal{O}(v)$ is positive definite, since we have shown the existence of v^*, the minimizer of $J(v)$.

(b) We recall the search vector $s(v)$ in (4.22). By properties of the projection $\mathcal{P}_Q\{v\}$ in (4.15), we rephrase $s(v)$ as

$$s(v) = \theta(-\alpha_s \nabla J(v^k)),$$

where $\theta \in [0,1]$ is a parameter for pulling back the step size due to the implemented projection method. Thus, we can show that $\nabla V_\mathcal{O}(v)^T s(v) =$

$-\theta\alpha_s|\nabla J(v)|^2 < 0, \forall v \in Q\backslash\{v^*\}$, and $\nabla V_{\mathcal{O}}(v^*)^T s(v^*) = 0$, because it is either $\nabla J(v) = 0$ or $\theta = 0$ depending on whether v^* is at the boundary of Q.

(c) From the argument above, we can derive

$$\begin{aligned} |s(v)|^2 &= \theta^2\alpha_s^2|\nabla J(v)|^2 \\ &\leq \theta\alpha_s^2|\nabla J(v)|^2 \leq -\kappa_s \nabla V_{\mathcal{O}}(v)^T s(v), \end{aligned}$$

as long as we choose $\kappa_s \geq \alpha_s$.

(d) $\nabla V_{\mathcal{O}}(v)$ is Lipschitz, since $\nabla V_{\mathcal{O}}(v) = \nabla J(v)$ and recalling (4.26), it can be checked that $\nabla J(v)$ is C^1 on Q.

□

Next, we focus on the NES algorithm. Motivated in the previous discussion, we regard this algorithm as a perturbed optimizer, $\mathcal{O}_p$. Compared with (4.14), the imprecision of $\mathcal{O}_p$ appears in the approximation of $\nabla J(v^k)$ via (4.13), that is

$$\widehat{\nabla J}(v^k, z^k) = \frac{1}{\mu_s}(h(z^{k,1} + l(v^{k,1}), v^{k,1}) - h(z^k + l(v^k), v^k)), \tag{4.29}$$

where we denote $v^{k,1} = v^k + \mu_s$ and $z^{k,1} = x(t^{k,1}) - l(v^{k,1})$, and we also recall $z^k = x(t^k) - l(v^k)$ from Chapter 3 and $t^{k,1} = t^k + T$. We also note that by (4.25), with $v = v^{k,1}$, $z^{k,1}$ is related with z^k in the following way

$$\begin{aligned} z^{k,1} &= A(v^{k,1})(x^k - l(v^{k,1})) \\ &= A(v^{k,1})(x^k - l(v^k) + l(v^k) - l(v^{k,1})) \\ &= A(v^{k,1})(z^k + \Delta l), \end{aligned} \tag{4.30}$$

where we let $\Delta l = l(v^k) - l(v^{k,1})$. Therefore, we can describe $\mathcal{O}_p$ as

$$\mathcal{O}_p : \begin{array}{l} v^{k+1} = v^k + s_p(v^k, z^k), \\ s_p(v^k, z^k) = \mathcal{P}_Q\{v^k - \alpha_s \widehat{\nabla J}(v^k, z^k)\} - v^k. \end{array}$$

Before characterizing the properties of $\mathcal{O}_p$, we first need to explore a simpler case—when the projection method is not present. By referring to equations (4.11) and (4.13), we use the following notation to represent the basic gradient-descent optimizer without projection, that is

$$\mathcal{O}_b : \begin{array}{l} v^{k+1} = v^k + s_b(v^k), \\ s_b(v^k) = -\alpha_s \nabla J(v^k), \end{array} \tag{4.31}$$

$$\mathcal{O}_{b,p} : \begin{array}{l} v^{k+1} = v^k + s_{b,p}(v^k, z^k), \\ s_{b,p}(v^k, z^k) = -\alpha_s \widehat{\nabla J}(v^k, z^k). \end{array} \tag{4.32}$$

Lemma 4.3.5. *($s_{b,p}(v^k, z^k)$ satisfies Assumption 3.1.4, and existence of κ_Σ in Assumption 3.1.6): The term, $s_{b,p}(v^k, z^k)$ can be expressed by*

$$s_{b,p}(v^k, z^k) = s_b(v^k) + p_b(z^k), \tag{4.33}$$

satisfying Assumption 3.1.4 on the additive perturbation. Also, there exists a $\Gamma > 0$ such that κ_Σ given by

$$\kappa_\Sigma \geq \frac{\Gamma}{\lambda_{min}(P)},$$

satisfies Assumption 3.1.6 on the vanishing perturbation, where $\lambda_{min}(P)$ is the minimum eigenvalue of P, as stated in $V_\Sigma(z)$ in (4.27).

Proof. We plug (4.29) into $s_{b,p}(v^k, z^k)$ in (4.32), which yields

$$s_{b,p} = -\frac{\alpha_s}{\mu_s}(h(z^{k,1} + l(v^{k,1}), v^{k,1}) - h(z^k + l(v^k), v^k)), \tag{4.34}$$

where we omit the arguments of $s_{b,p}(v^k, z^k)$. Furthermore, if we let

$$f_1(x) = h(x, v)|_{v \text{ is fixed at } v^k},$$
$$f_2(x) = h(x, v)|_{v \text{ is fixed at } v^{k,1}},$$

and apply Lemma 3.2.2, we get

$$h(z^k + l(v^k), v^k) = h(l(v^k), v^k) + I_1,$$
$$h(z^{k,1} + l(v^{k,1}), v^{k,1}) = h(l(v^{k,1}), v^{k,1}) + I_2,$$

where

$$I_1 = \int_0^1 \left(\frac{\partial h}{\partial x}(v^k, \tau_1 z^k + l(v^k)) \right)^T z^k \, \mathrm{d}\tau_1,$$
$$I_2 = \int_0^1 \left(\frac{\partial h}{\partial x}(v^{k,1}, \tau_2 z^{k,1} + l(v^{k,1})) \right)^T z^{k,1} \, \mathrm{d}\tau_2.$$

Thus, by recalling $J(v) = h(l(v), v)$, equation (4.34) yields

$$s_{b,p} = -\frac{\alpha_s}{\mu_s}(J(v^{k,1}) - J(v^k) + I_2 - I_1).$$

In addition, applying Lemma 3.2.2 similarly on $J(v^{k,1}) = J(v^k + \mu_s)$, we get

$$J(v^{k,1}) = J(v^k) + \int_0^1 \nabla J(v^k + \tau_3 \mu_s)\mu_s \, \mathrm{d}\tau_3,$$

which yields

$$s_{b,p} = -\alpha_s \left(\nabla J(v^k) + I_3 + \frac{I_2}{\mu_s} - \frac{I_1}{\mu_s} \right), \tag{4.35}$$

wherein

$$I_3 = -\nabla J(v^k) + \int_0^1 \nabla J(v^k + \tau_3 \mu_s) \, \mathrm{d}\tau_3.$$

Then, we recall from (4.7) that $h(x, v)$ has a quadratic form with respect to x. Thus, it can be represented by

$$h(x, v) = x^T H(v) x,$$

with

$$H(v) = \begin{bmatrix} -\frac{1}{2}v\omega^2 & 0 \\ 0 & -\frac{1}{2}v \end{bmatrix},$$

which also implies

$$\frac{\partial h}{\partial x}(x, v) = 2H(v)x.$$

Therefore, I_1 and I_2 can be computed in the following way, where we note that $H(v)$ is a symmetric matrix:

$$\begin{aligned} I_1 &= \int_0^1 (2H(v^k)(l(v^k) + \tau_1 z^k))^T z^k \, \mathrm{d}\tau_1 \\ &= 2l(v^k)^T H(v^k) z^k + (z^k)^T H(v^k) z^k; \end{aligned} \tag{4.36}$$

similarly,

$$I_2 = 2l(v^{k,1})^T H(v^{k,1}) z^{k,1} + (z^{k,1})^T H(v^{k,1}) z^{k,1}.$$

We then recall equation (4.30), thereby, I_2 can be derived as

$$\begin{aligned} I_2 =& 2l(v^{k,1})^T H(v^{k,1}) A(v^{k,1})(z^k + \Delta l) \\ &+ (z^k + \Delta l)^T A(v^{k,1})^T H(v^{k,1}) A(v^{k,1})(z^k + \Delta l). \end{aligned}$$

Further, for notational simplicity, let us denote $R(v^{k,1}) \triangleq 2l(v^{k,1})^T H(v^{k,1}) A(v^{k,1})$ and $S(v^{k,1}) \triangleq A(v^{k,1})^T H(v^{k,1}) A(v^{k,1})$, whereby we note that $R(v^{k,1}) \in \mathbb{R}^{1\times 2}$, $S(v^{k,1}) \in \mathbb{R}^{2\times 2}$; then, I_2 can be further derived as

$$\begin{aligned} I_2 &= R(v^{k,1})(z^k + \Delta l) + (z^k + \Delta l)^T S(v^{k,1})(z^k + \Delta l) \\ &= R(v^{k,1}) z^k + R(v^{k,1}) \Delta l + (z^k)^T S(v^{k,1}) z^k \\ &+ (z^k)^T S(v^{k,1}) \Delta l + (\Delta l)^T S(v^{k,1}) z^k + (\Delta l)^T S(v^{k,1}) \Delta l. \end{aligned}$$

We hereby note that $S(v^{k,1})$ is a symmetric matrix and that $(z^k)^T S(v^{k,1}) \Delta l$ is scalar-valued, which implies

$$(z^k)^T S(v^{k,1}) \Delta l = ((z^k)^T S(v^{k,1}) \Delta l)^T = (\Delta l)^T S(v^{k,1}) z^k.$$

Therefore, I_2 can be further expressed as

$$\begin{aligned} I_2 =& (R(v^{k,1}) + 2(\Delta l)^T S(v^{k,1})) z^k + (z^k)^T S(v^{k,1}) z^k \\ &+ R(v^{k,1}) \Delta l + (\Delta l)^T S(v^{k,1}) \Delta l. \end{aligned}$$

We then plug this latter equation, together with (4.36), back in equation (4.35) and also recall $s_b(v^k)$ from (4.31); thereby, we get

$$s_{b,p} = s_b(v^k) + p_b(z^k), \tag{4.37}$$

where the perturbation $p_b(z^k)$ is continuous and takes the following form

$$p_b(z^k) = C_1 z^k + (z^k)^T C_2 z^k + C_3, \tag{4.38}$$

wherein $C_1 \in \mathbb{R}^{1\times 2}$, $C_2 \in \mathbb{R}^{2\times 2}$, and $C_3 \in \mathbb{R}$, whose explicit forms are described as follows

$$\begin{aligned}
C_1 &= \frac{\alpha_s}{\mu_s}(2l(v^k)^T H(v^k) - R(v^{k,1}) - 2(\Delta l)^T S(v^{k,1})),\\
C_2 &= \frac{\alpha_s}{\mu_s}(H(v^k) - S(v^{k,1})),\\
C_3 &= \frac{\alpha_s}{\mu_s}(-R(v^{k,1})\Delta l - (\Delta l)^T S(v^{k,1})\Delta l) - \alpha_s I_3.
\end{aligned}$$

We then note that by (4.37) and (4.38), Assumption 3.1.4 is satisfied.

Next, we will show that $p_{b,v}(z^k)$, the vanishing component of $p_b(z^k)$,satisfies the inequality in Assumption 3.1.6 with proper choice of κ_Σ. Directly by (4.38), we can see

$$p_{b,v}(z^k) = C_1 z^k + (z^k)^T C_2 z^k,$$

which, by applying $|a+b|^2 \leq 2(|a|^2 + |b|^2)$ inequality, we can derive to be

$$\begin{aligned}
|p_{b,v}(z^k)|^2 &\leq 2(|C_1 z^k|^2 + |{z^k}^T C_2 z^k|^2)\\
&\leq 2(\|C_1\|^2 |z^k|^2 + \|C_2\|^2 |z^k|^4). \qquad (4.39)
\end{aligned}$$

Let us also denote $\Gamma \triangleq \max\{2\|C_1\|^2, 2\|C_2\|^2\}$, then by (4.39), we obtain

$$|p_{b,v}(z^k)|^2 \leq \Gamma(|z^k|^2 + |z^k|^4). \qquad (4.40)$$

Besides, recalling $V_\Sigma(z^k) = (z^k)^T P z^k + ((z^k)^T P z^k)^2$ and that $\lambda_{\text{min}}(P) > 1$, by Lemma 4.3.2, we get

$$\begin{aligned}
V_\Sigma(z^k) &\geq \lambda_{\text{min}}(P)|z^k|^2 + \lambda_{\text{min}}^2(P)|z^k|^4\\
&\geq \lambda_{\text{min}}(P)(|z^k|^2 + |z^k|^4). \qquad (4.41)
\end{aligned}$$

By comparing (4.40) and (4.41), we note that choosing $\kappa_\Sigma \geq \frac{\Gamma}{\lambda_{\text{min}}(P)}$ verifies $\kappa_\Sigma V_\Sigma \geq |p_{b,v}|^2$, i.e., it verifies Assumption 3.1.6. The proof is then complete. $\square$

The following result accounts for the properties of the search vector $s_p(v^k, z^k)$ for $\mathcal{O}_p$, when the projection method is used.

Proposition 4.3.6. *($s_p(v^k, z^k)$ satisfies Assumption 3.1.4, and existence of κ_Σ in Assumption 3.1.6): The term, $s_p(v^k, z^k)$ can be expressed by*

$$s_p(v^k, z^k) = s(v^k) + p(z^k),$$

satisfying Assumption 3.1.4 on the additive perturbation. Also, there exists a real number $\kappa_\Sigma > 0$ satisfying Assumption 3.1.6 on the vanishing perturbation.

Proof. First, we describe $s_p(v^k, z^k)$ as

$$s_p(v^k, z^k) = \mathcal{P}_Q\{v^k + s_{b,p}(v^k, z^k)\} - v^k.$$

Then, recalling $s(v^k) = \mathcal{P}_Q\{v^k + s_b(v^k)\} - v^k$, we get

$$s_p(v^k, z^k) = s(v^k) + p(z^k),$$

with

$$p(z^k) = \mathcal{P}_Q\{v^k + s_{b,p}(v^k, z^k)\} - \mathcal{P}_Q\{v^k + s_b(v^k)\},$$

where we note that $p(z)$ is continuous on z.

We then recall from Remark 3.1.5 about the vanishing component $p_v(z^k)$ that

$$\begin{aligned} p_v(z^k) &= p(z^k) - p(0) \\ &= \mathcal{P}_Q\{v^k + s_{b,p}(v^k, z^k)\} - \mathcal{P}_Q\{v^k + s_{b,p}(v^k, 0)\}. \end{aligned}$$

Then, by non-expansive property of projection method [3], we have

$$|p_v(z^k)| \le |s_{b,p}(v^k, z^k) - s_{b,p}(v^k, 0)|,$$

which then by (4.33), gives

$$|p_v(z^k)| \le |p_b(z^k) - p_b(0)| = |p_{b,v}(z^k)|.$$

This implies the κ_Σ characterized in Lemma 4.3.5 is also valid for the case when projection is present, since

$$\kappa_\Sigma V_\Sigma(z^k) \ge |p_{b,v}(z^k)|^2 \ge |p_v(z^k)|^2.$$

This completes the proof. ☐

Theorem 4.3.7. *(Stability of the WEC and NES interconnection): Let $\mathcal{A}(v)$ denote the map from v to its associated limit cycle* (4.16). *Consider the system* (4.10)$-$(4.22), *the maximizer $v^* \in Q$, together with the associated limit cycle $\mathcal{A}(v^*)$, is* semiglobally practically asymptotically stable *in the sense that the system* (4.25)$-$(4.22) *is semiglobally practically asymptotically stable at $(0^T, (v^*)^T)^T$, where* (4.25) *is obtained from* (4.10) *by the Poincaré map* (4.18) *and the state transformation* (4.24).

Proof. Previously in this section, for the interconnection of (4.25) and (4.22), we have verified Assumptions 3.1.1 and 3.1.3 on the Lyapunov functions V_Σ and $V_\mathcal{O}$, Assumptions 3.1.7 on the Lipschitz property of l, and Assumptions 3.1.4 and 3.1.6 on the properties of the perturbation to the search vector; thus, as the consequence of Theorem 3.2.4 and 3.2.5, the point $(0^T, (v^*)^T)^T$ is semiglobally practically asymptotically stable. Furthermore, we recall that the plant (4.25) is obtained from (4.10) by the Poincaré map (4.18) and the state transformation (4.24). Therefore, we complete the proof. $\square$

Chapter 4, in part, has been submitted for publication of the material as it may appear in proceedings of the 2014 American Control Conference, Portland, OR, June 2014, Tianjia Chen, Hamed Foroush and Sonia Martinez. The thesis author was the primary investigator and author of this paper.

Chapter 5

Simulations

In this chapter, we illustrate the performance of the NES algorithm in solving the power maximization problem of the point-absorber WEC as formulated in Chapter 2 and as discussed in Chapter 4. In addition, we also implement the sampled-data extremum-seeking scheme on irregular-wave condition, where the simulation results have demonstrated the functionality and practicality of the proposed approach.

5.1 Regular-Wave Condition

Table 5.1: The dataset used in the simulations for regular-wave condition

Quantity	Symbol	Unit	Value
Mass $(M_s + M_a)$	M	1×10^3kg	500
Hydraulic damping	D_h	1×10^3kg/s	30
Stiffness $(K_h + K_p)$	K	1×10^3N/m	750
Wave frequency	ω	rad/s	1.2
Wave excitation force	F	1×10^3N	200

We use a set of parameters similar to those in [13], which are aggregated in Table 5.1. Two representative results are included in Figures 5.1 and 5.2. Referring to NES algorithm stated in Algorithm Table 1, in both these cases, v_0 is chosen to be $v_0 = 20$, the step-size $\alpha_s = 5$, the step-size in the Euler method

$\mu_s = 0.1$, and the waiting time $T = 60\,\mathrm{sec}$. The difference between these cases lies in the considered constraint set. Recall the optimization problem formulated in Chapter 2

$$\max_{v \in Q} P^{ss}_{\text{avg}}(v),$$
$$\text{s.t. } (2.6),$$

where the optimizer v^* can be computed by leveraging the following equation from Lemma 4.1.1:

$$P^{ss}_{\text{avg}}(v) = \frac{1}{2}\frac{\omega^2 F^2 v}{(K - M\omega^2)^2 + (D_h + v)^2\omega^2}.$$

For the first case, the maximizer v^* is given as $v^* = \sqrt{D_h^2\omega^2 + (K - M\omega^2)^2}/\omega = 39.05$ with the constraint set $Q_1 = [0, 45]$, while for the second case, $v^* = v^{\max} = 30$ due to the constraint set $Q_2 = [0, 30]$.

In each figure, plots (a) and (c) show, respectively, how the control variable $v = D_p$ converges to a neighborhood of v^* and that the averaged power-output P_{avg} is thereby maximized. The units for D_p and P_{avg} are 1×10^3kg/s and Kilowatt, respectively. The red dashed line indicates the value of $v^{\max}$. In order to show the convergence of the state trajectory to the limit cycle $\mathcal{A}(v^*)$, we provide plots (b) and (d). Plot (b) is the plot of the limit cycle $\mathcal{A}(v^*)$, which is an ellipse for both cases. Plot (d) depicts how the distance from the state to the limit cycle $\mathcal{A}(v^*)$ converges to zero, where the distance, d, is characterized as $d \triangleq d(x, \mathcal{A}(v^*)) = \inf_{a \in \mathcal{A}(v^*)} |x - a|$.

The simulation results show that the NES algorithm is capable of solving the power maximization problem while ensuring the system stability. This is in perfect accordance with the discussion in Chapter 4.

5.2 Irregular-Wave Condition

The irregular waves can be obtained by linear superposition of regular waves, with some randomness on the phase of each components. We model the

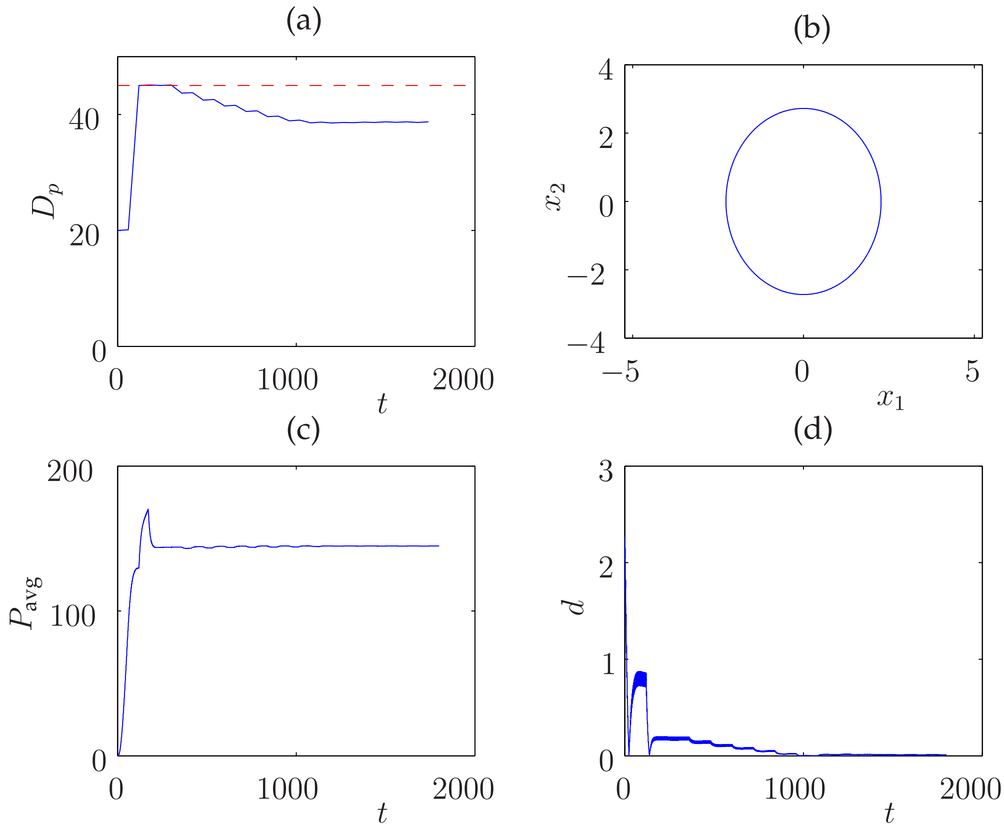

Figure 5.1: Simulation for regular-wave condition: case 1

irregular waves in a similar manner with [7].

Noticeably, for irregular-wave condition, the output map we consider for the regular-wave case may not be eligible, since it relies on the measurement or estimation of the wave frequency. Instead, we can choose a more practical output map, which is simply the measured average power output of the plant over some certain past period of time.

Table 5.2: The dataset used in the simulation for irregular-wave condition

Quantity	Symbol	Unit	Value
Mass $(M_s + M_a)$	M	1×10^3kg	600
Hydraulic damping	D_h	1×10^3kg/s	30
Stiffness $(K_h + K_p)$	K	1×10^3N/m	640
Wave frequency	ω	rad/s	1
Wave excitation force	F	1×10^3N	200

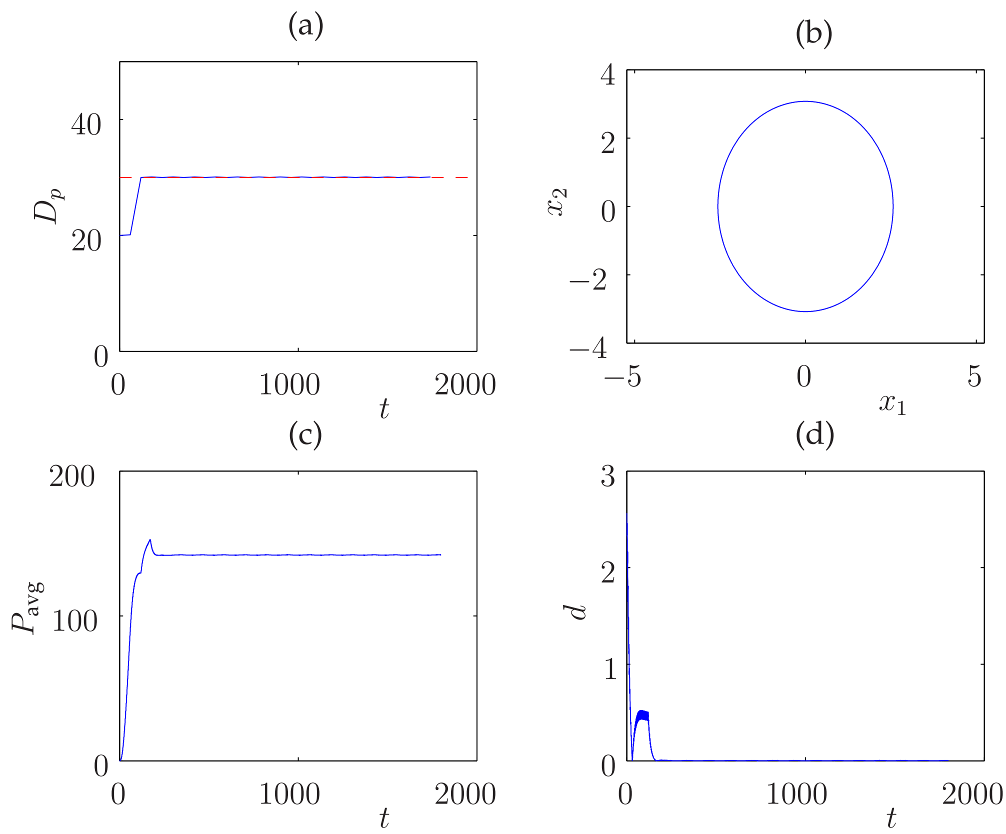

Figure 5.2: Simulation for regular-wave condition: case 2

The dataset for the WEC plant we have used is shown in Table 5.2. Also, the simulation result can be seen in Figure 5.3. We still keep $v_0 = 20$ as a starting point. In addition, to cope with the irregularity of the wave, we reset the parameters of the NES algorithm: the step-size $\alpha_s = 20$, the step-size in the Euler method $\mu_s = 5$, and the waiting time $T = 2000\,\text{sec}$. In order to emphasize the functionality of the extremum-seeking approach, we have removed the constraint set for this case. Same as the regular-wave case, the units for D_p and P_{avg} are 1×10^3kg/s and Kilowatt, respectively. We can observe from Figure 5.3 that the NES, with appropriate choice of the parameters, is capable for working in the irregular-wave condition.

Chapter 5, in part, has been submitted for publication of the material as it may appear in proceedings of the 2014 American Control Conference, Portland,

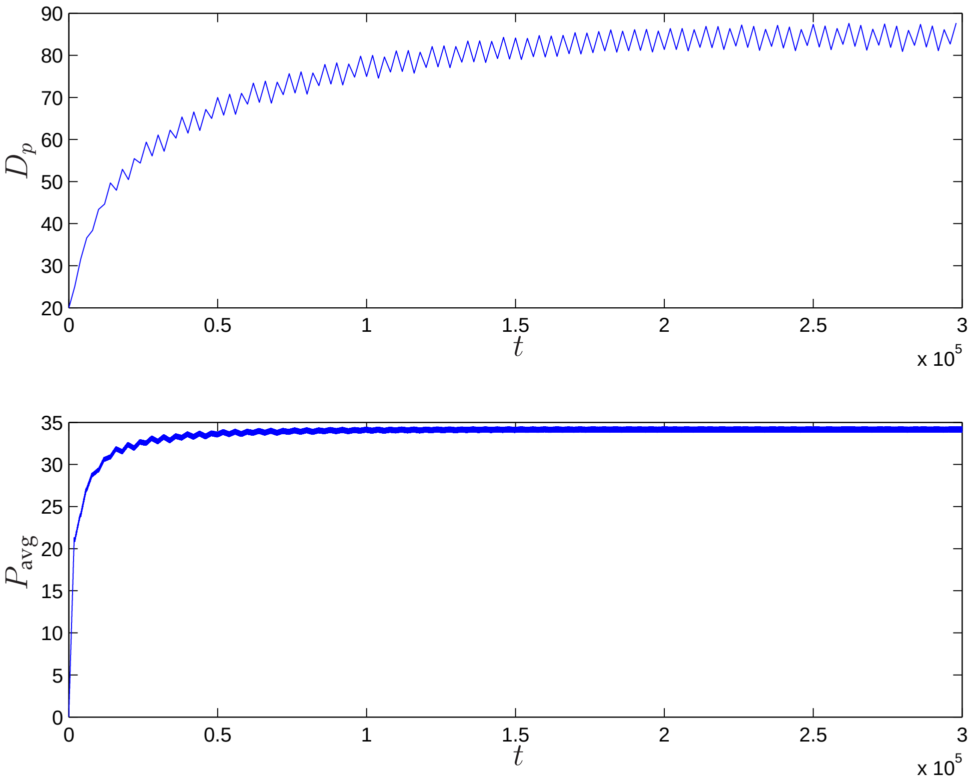

Figure 5.3: Simulation for irregular-wave condition

OR, June 2014, Tianjia Chen, Hamed Foroush and Sonia Martinez. The thesis author was the primary investigator and author of this paper.

Chapter 6

Conclusions

In this thesis, we have studied the application of a sampled-data ES approach to maximize the power extraction in WECs modeled as point-absorbers where the control parameter is the PTO damping, the value of which should be constrained in a compact set.

We have first reviewed the relevant sampled-data ES theory, where we have adapted its framework to account for discrete-time class of systems and constrained control inputs. The motivation of doing such adaptation is that the analysis of the stability regarding the WEC model involves the stability of a limit cycle, which can be interpreted as the stability of the related Poincaré map. Then, we have proposed our NES algorithm which solves the optimization problem of power extraction and ensures the stability of the system. Accordingly, we have also proved the functionality of the NES algorithm by applying the adapted sampled-data ES theory, where we have employed the Poincaré map technique to convert the original system to a discrete-time one. The simulation results have shown the capability of the proposed sampled-data extremum-seeking scheme to maximize the power output, under both the regular- and irregular-wave condition.

In future work, we would like to focus on the applicability of this methodology to alternative output maps and WEC mechanisms. Upon the successful simulation on the irregular-wave case, we would also like to explore the analytical work for that scenario.

Bibliography

[1] K.B. Ariyur and M. Krstic. *Real-Time Optimization by Extremum-Seeking Control*. Wiley-interscience publication. John Wiley & Sons, 2003.

[2] G. D. Backer. *Hydrodynamic design optimization of wave energy converters consisting of heaving point absorbers*. PhD thesis, Ghent University, Belgium, 2009.

[3] D. P. Bertsekas. *Nonlinear programming*. Athena Scientific, 1999.

[4] K. Budal and J. Falnes. Interacting point absorbers with controlled motion. *Power from sea waves*, pages 381–399, 1980.

[5] B. Drew, A. R. Plummer, and M. N. Sahinkaya. A review of wave energy converter technology. *Proceedings of the Institution of Mechanical Engineers, Part A: Journal of Power and Energy*, 223(8):887–902, 2009.

[6] A.F.O. Falcão. Wave energy utilization: A review of the technologies. *Renewable and Sustainable Energy Reviews*, 14(3):899–918, 2010.

[7] P. B. Garcia-Rosa, F. Lizarralde, and S. F. Estefen. Optimization of the wave energy absorption in oscillating-body systems using extremum seeking approach. In *American Control Conference*, pages 1011–1016, 2012.

[8] S. Z. Khong, D. NešIć, Y. Tan, and C. Manzie. Unified frameworks for sampled-data extremum seeking control: Global optimisation and multi-unit systems. *Automatica*, 49(9):2720–2733, 2013.

[9] U. A. Korde. Efficient primary energy conversion in irregular waves. *Ocean engineering*, 26(7):625–651, 1999.

[10] U. A. Korde. Control system applications in wave energy conversion. In *OCEANS 2000 MTS/IEEE Conference and Exhibition*, volume 3, pages 1817–1824. IEEE, 2000.

[11] K. Kvaternik and L. Pavel. Interconnection conditions for the stability of nonlinear sampled-data extremum seeking schemes. In *IEEE Int. Conf. on Decision and Control and European Control Conference*, pages 4448–4454. IEEE, 2011.

[12] A.R. Plummer and M. Schlotter. Investigating the performance of a hydraulic power take-off. In *European Wave and Tidal Energy Conference*, 2009.

[13] M. Santos, E. Tedeschi, P. Ricci, M. Molinas, and J.L. Martin. Grid connection improvements by control strategy selection for wave energy converters. *Proc. ICREPQ2011*, 1:446–448, 2011.

[14] E. Tedeschi and M. Molinas. Tunable control strategy for wave energy converters with limited power takeoff rating. *IEEE Transactions on Industrial Electronics*, 59(10):3838 – 3846, 2012.

[15] A.R. Teel and D. Popovic. Solving smooth and nonsmooth multivariable extremum seeking problems by the methods of nonlinear programming. In *American Control Conference*, volume 3, pages 2394–2399. IEEE, 2001.

[16] F. Verhulst. *Nonlinear differential equations and dynamical systems*. Springer verlag, 1996.

[17] C. Zhang and R. Ordóñez. *Extremum-Seeking Control and Applications: A Numerical Optimization-Based Approach*. Springer, 2011.

[18] Z. Zhang, X. Bao, C.D. Rennie, I. Nistor, and A. Cornett. Water wave frequency detection by optical fiber sensor. *Optics Communications*, 281(24):6011 – 6015, 2008.